

Entanglement Negativity and Mutual Information after a Quantum Quench: Exact Link from Space-Time Duality

Bruno Bertini,^{1,2} Katja Klobas,³ and Tsung-Cheng Lu⁴

¹*School of Physics and Astronomy, University of Nottingham, Nottingham, NG7 2RD, UK*

²*Centre for the Mathematics and Theoretical Physics of Quantum Non-Equilibrium Systems, University of Nottingham, Nottingham, NG7 2RD, UK*

³*Rudolf Peierls Centre for Theoretical Physics, Clarendon Laboratory, Oxford OX1 3PU, UK*

⁴*Perimeter Institute for Theoretical Physics, Waterloo, Ontario N2L 2Y5, Canada*

(Dated: April 1, 2022)

We study the growth of entanglement between two adjacent regions in a tripartite, one-dimensional many-body system after a quantum quench. Combining a replica trick with a space-time duality transformation, we derive an exact, universal relation between the entanglement negativity and Rényi-1/2 mutual information which holds at times shorter than the sizes of all subsystems. Our proof is directly applicable to *any* translationally invariant local quantum circuit, i.e., any lattice system in discrete time characterised by local interactions, irrespective of the nature of its dynamics. Our derivation indicates that such a relation can be directly extended to any system where information spreads with a finite maximal velocity.

The Hilbert space of a quantum many-body system is frighteningly large. The number of components required to specify a vector in this space scales exponentially with the size of the system, and therefore, in practice one can encode the whole Hilbert space only for small sizes. Fortunately, in most physically relevant systems knowledge of the full Hilbert space is not necessary to describe equilibrium physics. Indeed, the latter is encoded in a relatively small family of states characterised by low quantum entanglement [1]. These states are efficiently described by the so-called *tensor-network techniques* [2, 3], which are particularly effective in one spatial dimension.

The situation changes drastically for systems driven out of equilibrium. Even if the initial state admits an efficient description, generic quantum dynamics inevitably leads to growth of entanglement [4–16], which severely obstructs the simulability of systems at intermediate time scales. However, at sufficiently long times the systems are expected to achieve (generalised) thermalisation [17–22], where the reduced density matrix of a subregion becomes equivalent to an equilibrium ensemble consistent with the local conservation laws of the time-evolution operator [22, 23]. Therefore, the long-time-evolved state of a subsystem has small mixed-state entanglement and admits an efficient description in terms of a matrix product operator (MPO) [24, 25]. As a consequence, one expects the amount of resources required to encode a time-evolving quantum many-body state grows at early times, and decays at long times.

This phenomenon has been described as *entanglement barrier* [26, 27], and has attracted substantial attention due to the ongoing effort to simulate quantum dynamics for intermediate times [28–37]. The study of the entanglement barrier is not only relevant for quantifying the computational cost, but can also be used to characterise the nature of the non-equilibrium dynamics in a universal manner. For instance, the shape of the entanglement barrier has been shown to be qualitatively different for integrable and chaotic dynamics [27, 38].

Due to its relevance for numerical simulations, the entanglement barrier has been typically probed by means of the so-called *operator space entanglement entropy* [39, 40]. Loosely speaking, this quantity estimates the numerical cost to achieve a faithful MPO representation of the reduced density matrix [26, 39, 40]. Nevertheless, it is not a measure of mixed-state entanglement. For instance, separable mixed states can have non-zero operator-space entanglement entropy [26, 39].

In this Letter we adopt a more general quantum-information-theoretical point of view and study the entanglement barrier through the lens of genuine mixed-state entanglement. Namely, we characterise the entanglement dynamics of the reduced density matrix of a finite subsystem using entanglement negativity [41–45], which has been a useful tool to explore several universal aspects of many-body physics including conformal field theories [46–51], topologically ordered phases [52–58], as well as quantum dynamics [59–72].

Specifically, we study the dynamics of the negativity between the regions A and B under a tripartition ABC in *generic* one-dimensional systems with discrete space-time and local interactions, i.e., local quantum circuits. Combining a replica trick [46, 50] with a space-time duality approach [14–16, 73–85], we provide a simple expression for the negativity, which is applicable for times smaller than the sizes of the regions A, B, C . We then use this expression to show that, up to exponentially small corrections, the negativity coincides with the Rényi-1/2 mutual information divided by two. This result holds for *any* local quantum circuit with translation symmetry in space, irrespective of the nature of the dynamics. Our findings generalise those of Ref. [64] (see also [66, 67, 69, 70]), where the aforementioned relation between negativity and Rényi-1/2 mutual information was discovered in non-interacting systems, and argued to hold for all integrable systems.

More specifically, we consider a quantum quench from a pure state $|\Psi_0\rangle$ in a homogeneous local quantum cir-

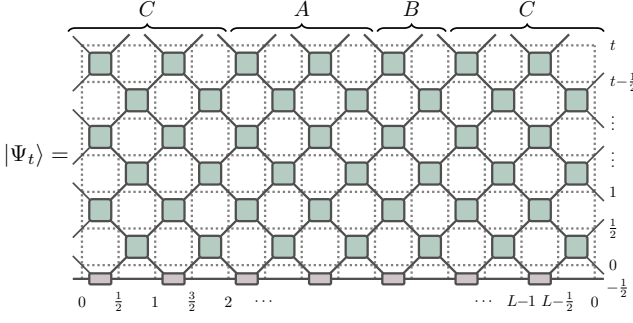


FIG. 1. Illustration of time-evolution in a brick-work quantum circuit. The initial state $|\Psi_0\rangle$ is assumed to be a two-site MPS (cf. Eq. (2)). Each time-step consists of applying two-site gates first to odd, and then to even pairs of consecutive sites, so that at time t the state is given by $|\Psi_t\rangle = \mathbb{U}^t |\Psi_0\rangle$, with \mathbb{U} defined in Eq. (1). The boundary conditions are assumed to be *periodic* (i.e., the site L is identified with the site 0), and the time-labels go from 0 to t in increments of $\frac{1}{2}$. For convenience we label the auxiliary degree of freedom of the initial MPS with $-\frac{1}{2}$.

cuit of $2L$ qudits (see Fig. 1), namely, a system where both space and time are discrete, each local site (labelled by integer and half-odd-integer numbers) hosts a d -state qudit, and there is a strict maximal speed v_{\max} for the propagation of signals.

Even though our argument is fully general and does not depend on the specific implementation of the circuit, for the sake of clarity we consider a brick-work quantum circuit where the time-evolution operator \mathbb{U} is written as

$$\mathbb{U} = \prod_{x \in \mathbb{Z}_L} \eta_x(U) \prod_{x \in \mathbb{Z}_L + \frac{1}{2}} \eta_x(U). \quad (1)$$

U denotes the *local gate*, i.e., a $d \times d$ unitary matrix specifying the interactions between two neighbouring qudits, and the *positioning operator* $\eta_x(\cdot)$ is a linear map that places a generic local operator O on a periodic chain of $2L$ qudits such that its right edge is at position x . This choice of units implies $v_{\max} = 1$.

To match the geometry of the circuit we consider an initial state of the form

$$|\Psi_0\rangle = \sum_{s_1, \dots, s_{2L}=1}^d \text{tr}[W^{s_1 s_2} \dots W^{s_{2L-1} s_{2L}}] |s_1\rangle \otimes \dots \otimes |s_{2L}\rangle, \quad (2)$$

where W^{sr} are $\chi \times \chi$ matrices (χ is an arbitrary positive integer) with matrix elements $W_{\mu\nu}^{sr}$, and $\{|s\rangle\}_{s=1}^d$ is the canonical orthonormal basis of \mathbb{C}^d . Namely, $|\Psi_0\rangle$ is a two-site matrix-product state (MPS) with *bond dimension* χ . Here we consider the usual case where the *MPS transfer matrix* τ , given by the following matrix elements,

$$\tau_{\mu_1 \nu_1}^{\mu_2 \nu_2} = \sum_{s_1, s_2=1}^d W_{\mu_1 \mu_2}^{s_1 s_2} (W_{\nu_1 \nu_2}^{s_1 s_2})^*, \quad (3)$$

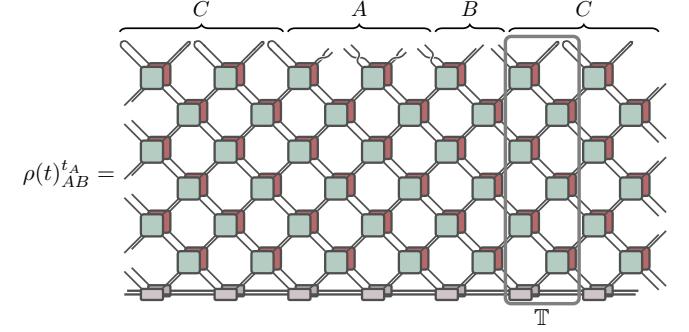


FIG. 2. ‘Folded’ representation of the partial transpose of the reduced density matrix, $\rho(t)_{AB}^{tA} = (\text{tr}_C |\Psi_t\rangle\langle\Psi_t|)^{tA}$. To obtain this diagram, we start with a copy of the state $|\Psi_t\rangle$ (green, cf. Fig. 1), and its Hermitian conjugate $\langle\Psi_t|$ (red), which is flipped and positioned behind $|\Psi_t\rangle$, i.e., the diagram is *folded* in half. The degrees of freedom in the subsystem C are then traced out, which is represented by connecting the legs of the two copies. Finally, we perform the partial transpose $(\cdot)_{AB}^{tA}$, which amounts to exchanging the output legs of the two copies in the subsystem A (hence the twist).

has a unique maximal eigenvalue (which we set to 1).

In the following, we consider two adjacent, finite, and non-complementary regions A and B in a tripartite system ABC (see Fig. 1), and characterise the entanglement between A and B via *logarithmic negativity* [41–44]

$$\mathcal{E}(t) := \ln \text{tr}[\rho(t)_{AB}^{tA}], \quad (4)$$

where $\rho(t)_{AB} = \text{tr}_C |\Psi_t\rangle\langle\Psi_t|$ is the reduced density matrix of the subsystem $A \cup B$ at time t and $(\cdot)_{AB}^{tA}$ represents the partial transpose with respect to A .

Our first objective is to obtain a more convenient expression for Eq. (4). To this end we proceed in two steps. First, we employ the replica trick by considering the even moments of the partially transposed density matrix [46, 50]

$$\mathcal{E}_{2n}(t) := \ln \text{tr}[(\rho(t)_{AB}^{tA})^{2n}] \quad (5)$$

for any positive integer n , which can then be reduced to the logarithmic negativity via an analytic continuation: $2n \mapsto \alpha$ followed by the limit $\alpha \rightarrow 1$.

Second, we note that the quantities defined in Eq. (5) can be conveniently computed using the space-time duality approach for the entanglement dynamics of Ref. [14] (see also [15, 16]), see Fig. 2 for a pictorial representation. We begin by introducing the *space transfer matrix*

$$\mathbb{T} = \mathbb{O} \cdot (\tilde{\mathbb{U}} \otimes \tilde{\mathbb{U}}^*) \in \text{End}(\mathcal{H}_t^2), \quad (6)$$

where $(\cdot)^*$ represents complex conjugation, $\mathcal{H}_t = \mathbb{C}^{d^{2t+1}}$ denotes the Hilbert space of $2t+1$ qudits together with the initial MPS auxiliary space, \mathbb{O} denotes the operator coupling the two copies of time-evolution,

$$\mathbb{O} := \sum_{r,s=1}^d \tilde{\eta}_t(|r\rangle\langle s|) \otimes \tilde{\eta}_t(|r\rangle\langle s|), \quad (7)$$

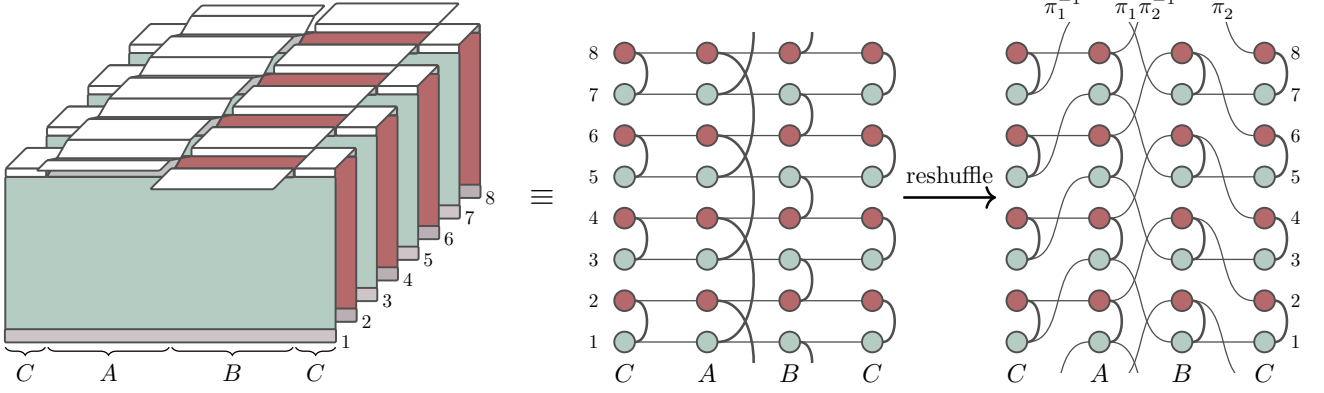


FIG. 3. Schematic illustration of $\exp[\mathcal{E}_{2n}(t)] = \text{tr}[(\rho(t)_{AB}^{t_A})^{2n}]$. In the left panel the green and red rectangles represent the time-evolved state and its conjugate respectively (i.e., a more schematic representation of the objects in Fig. 2), and the white connections show how the legs of the different copies are connected. For clarity we introduce a simplified representation in the middle panel, where each copy is now represented by a row, and each column corresponds to one of the subsystems (right-most and left-most columns coincide due to periodic boundary conditions). Connections are represented by thick black lines, while the thinner horizontal lines connect different subsystems within the same copy. In the rightmost panel we reshuffled the positions of different copies inside each subsystem, so that the connections always occur between nearest neighbours. This is achieved by performing a permutation of copies at each interface between different subsystems, as described in Eq. (10).

and $\tilde{\mathbb{U}}$ describes the evolution of one copy in the space direction,

$$\tilde{\mathbb{U}} := \left(\prod_{\tau \in \mathbb{Z}_t + \frac{1}{2}} \tilde{\eta}_\tau(\tilde{U}) \right) \left(\prod_{\tau \in \mathbb{Z}_t + 1} \tilde{\eta}_\tau(\tilde{U}) \right) \tilde{\eta}_0(\tilde{M}). \quad (8)$$

Here \tilde{U} and \tilde{M} are obtained from the local unitary gate U and the MPS matrix M by applying the spacetime-duality transformation $(\tilde{\cdot})$

$$[\tilde{O}]_{kl}^{ij} = O_{ki}^{lj}, \quad (9)$$

while $\tilde{\eta}_\tau(\cdot)$ denotes the “dual” positioning operator. The latter places a local operator in \mathcal{H}_t^2 , so that the *top* edge is at position τ (see Fig. 1 for the time and space coordinates). A direct interpretation of the space transfer matrix \mathbb{T} can be seen from Fig. 2: it is the evolution operator when one exchanges the roles of space and time.

Referring now to Fig. 3, Eq. (5) can be expressed in terms of the space transfer matrix \mathbb{T} as

$$\mathcal{E}_{2n} = \ln \text{tr}[(\mathbb{T}_{2n}^{(\pi_1)})^{L_A} (\mathbb{T}_{2n}^{(\pi_2)})^{L_B} (\mathbb{T}_{2n})^{L_C}], \quad (10)$$

where L_S denotes the number of sites in S divided by two and we introduced the operators

$$\mathbb{T}_m = \mathbb{T}^{\otimes m}, \quad \mathbb{T}_m^{(\sigma)} = \mathbb{P}_\sigma^\dagger \mathbb{T}_m \mathbb{P}_\sigma, \quad (11)$$

and the permutations

$$\begin{aligned} \pi_1 &= \begin{pmatrix} 1 & 2 & 3 & 4 & \cdots & 2m-1 & 2m \\ 2m-1 & 2 & 1 & 4 & \cdots & 2m-3 & 2m \end{pmatrix}, \\ \pi_2 &= \begin{pmatrix} 1 & 2 & 3 & 4 & \cdots & 2m-1 & 2m \\ 1 & 2m & 3 & 2 & \cdots & 2m-1 & 2m-2 \end{pmatrix}. \end{aligned} \quad (12)$$

Here, \mathbb{P}_σ is a unitary operator that acts on the multi-replica space \mathcal{H}_t^{2m} and reshuffles copies according to the permutation σ . Namely, its action is given by

$$\mathbb{P}_\sigma |\mathbf{s}_1\rangle \otimes \cdots \otimes |\mathbf{s}_{2m}\rangle = |\mathbf{s}_{\sigma(1)}\rangle \otimes \cdots \otimes |\mathbf{s}_{\sigma(2m)}\rangle, \quad (13)$$

where $|\mathbf{s}_j\rangle$ are basis states of \mathcal{H}_t . As pictured in Fig. 3 the rewriting in Eq. (10) essentially amounts to reordering the space-time sheets so that two copies connected by a contraction at the top are next to each other. Importantly, this is allowed only when the state $|\Psi_0\rangle$ is *pure*, otherwise space-time sheets are connected also to different copies at the bottom. In fact, this is the *only* ingredient needed for the validity of Eq. (10). No other property of the dynamics or the initial state has been used.

We now use the local structure of the dynamics to further simplify Eq. (10) in the early-time regime, i.e., when $v_{\max} t$ is smaller than the sizes of all subsystems A, B, C . First, due to the unitarity of the time evolution, \mathbb{T} has a unique maximal eigenvalue equal to one [74]. Second, the existence of the strict maximal speed v_{\max} of the propagation of signals implies (see, e.g., [86])

$$\mathbb{T}^x \simeq |\mathbf{r}\rangle\langle\mathbf{l}|, \quad x \geq v_{\max} t. \quad (14)$$

Here $|\mathbf{r}\rangle$ and $\langle\mathbf{l}|$ denote the *fixed points* of \mathbb{T} , i.e., the right/left eigenvectors corresponding to the eigenvalue one, and they are normalised to $\langle\mathbf{l}| \mathbf{r}\rangle = 1$. Moreover, we introduced the sign \simeq to indicate equality up to corrections of order $\mathcal{O}(\lambda^x)$, where λ is the subleading eigenvalue of the MPS transfer matrix defined in Eq. (3) (which coincides with \mathbb{T} when time t is zero). Thus, Eq. (14) becomes an exact equality in the limit $x \rightarrow \infty$. For non-infinite x , the exact equal sign holds for $\chi = 1$, i.e., when the initial state is a product state, or when the MPS transfer matrix has a single non-zero eigenvalue.

Eq. (14) admits a transparent physical interpretation: it states that the only correlations among regions out of the causal light cone are those present in the initial state (and decay exponentially in the distance due to the MPS form of the latter [3]). In the context of quantum many-body dynamics, Eq. (14) has first been utilised in Ref. [73] (see also [74, 75]) to develop a numerical algorithm to describe the dynamics of local observables for large system sizes. Recently, it gained renewed attention due to a number of interesting developments. Specifically, Refs. [14, 15, 86–88] showed that the fixed points can be determined exactly in certain non-trivial examples including both integrable quantum circuits, such as quantum cellular automaton Rule 54 [89, 90], and quantum chaotic ones, such as dual-unitary circuits [79]. Moreover, Refs. [14, 16] showed that the fixed points can be used to compute the slope of Rényi entropies following quantum quenches. Finally, Ref. [91–94] proposed a direct physical interpretation of the fixed points based on the Feynman-Vernon influence functional.

Used in our context, Eq. (14) implies that for

$$L_A, L_B, L_C \geq v_{\max} t, \quad (15)$$

Eq. (10) reduces to

$$\mathcal{E}_{2n}(t) \simeq \ln [\langle l_{2n} | \mathbb{P}_{\pi_1}^\dagger | r_{2n} \rangle \langle l_{2n} | \mathbb{P}_{\pi_1} \mathbb{P}_{\pi_2}^\dagger | r_{2n} \rangle \langle l_{2n} | \mathbb{P}_{\pi_2} | r_{2n} \rangle], \quad (16)$$

where we defined

$$|h_m\rangle = |h\rangle^{\otimes m}, \quad h = r, l. \quad (17)$$

To bring Eq. (16) to a form that can be analytically continued, we note that the states in $\mathcal{H}_t^{\otimes 2}$ can be viewed as matrices in $\text{End}(\mathcal{H}_t)$. Formally this is achieved by a vector-to-operator mapping defined on basis elements as (see, e.g., Ref. [78])

$$|s\rangle \otimes |r\rangle \longmapsto |s\rangle \langle r|. \quad (18)$$

In particular, we introduce the matrices M_l and M_r with the matrix elements

$$\langle s | M_h | r \rangle = (\langle s | \otimes \langle r |) |h\rangle, \quad h = l, r. \quad (19)$$

In this new language the constraint $\langle l | r \rangle = 1$ becomes

$$\text{tr}[M_l^\dagger M_r] = 1. \quad (20)$$

Using Eq. (19) to rewrite the matrix elements in Eq. (16) we find

$$\begin{aligned} \langle l_{2n} | \mathbb{P}_{\pi_1}^\dagger | r_{2n} \rangle &= \langle l_{2n} | \mathbb{P}_{\pi_2} | r_{2n} \rangle = \text{tr}[(M_l^\dagger M_r)^{2n}], \\ \langle l_{2n} | \mathbb{P}_{\pi_1} \mathbb{P}_{\pi_2}^\dagger | r_{2n} \rangle &= \text{tr}[(M_l^\dagger M_r)^n]^2. \end{aligned} \quad (21)$$

Therefore we arrive at the expression

$$\mathcal{E}_{2n}(t) \simeq 2 \ln \left(\text{tr}[(M_l^\dagger M_r)^{2n}] \text{tr}[(M_l^\dagger M_r)^n] \right), \quad (22)$$

valid in the regime given by Eq. (15). Now performing the analytic continuation $\mathcal{E}_{2n}(t) \mapsto \mathcal{E}_\alpha(t)$ followed by the limit $\alpha \rightarrow 1$, we find

$$\mathcal{E}(t) = \lim_{\alpha \rightarrow 1} \mathcal{E}_\alpha(t) \simeq 2 \ln \text{tr}[(M_l^\dagger M_r)^{1/2}], \quad (23)$$

where we implicitly used Eq. (20). This equation is our *first main result*: it gives a direct connection between the logarithmic negativity at early times and the fixed points of the space transfer matrix. In particular, it allows for an exact evaluation of the former in all cases where the fixed points are known exactly.

Crucially, even in the cases when the exact form of fixed points is not easily accessible, one can *always* use Eq. (23) to prove a universal relation between negativity and Rényi mutual information. To see this, let us again consider the tripartition in Fig. 1 and evaluate the Rényi mutual information

$$I_{A:B}^{(\alpha)}(t) := S_A^{(\alpha)}(t) + S_B^{(\alpha)}(t) - S_{AB}^{(\alpha)}(t), \quad (24)$$

where

$$S_S^{(\alpha)}(t) = \frac{1}{1-\alpha} \ln \text{tr}[\rho_S(t)^\alpha], \quad \alpha \in \mathbb{R}, \quad (25)$$

is the Rényi entropy of the subsystem S at time t .

As shown in Ref. [16], a space-time duality analysis along the lines of the one performed above gives

$$S_S^{(n)}(t) \simeq \frac{2}{1-n} \ln \text{tr}[(M_l^\dagger M_r)^n], \quad L_S, L_{\bar{S}} \geq v_{\max} t. \quad (26)$$

Comparing with Eq. (23), we then conclude that in the early-time regime described by Eq. (15), we have

$$2\mathcal{E}(t) \simeq I_{A:B}^{(1/2)}(t) \simeq S_A^{(1/2)}(t) \simeq S_B^{(1/2)}(t). \quad (27)$$

The universal relation (27) between negativity and Rényi mutual information (and Rényi entropies) at early times is our second main result. While for pure states this equivalence trivially follows from the definitions of the quantities involved, for mixed states it is highly non-trivial: negativity measures quantum entanglement while mutual information measures both quantum and classical correlations. Therefore, our results suggests that the correlation built by the dynamics between two subsystems A and B at early times is of purely quantum nature.

In fact, using Eq. (22) and Eq. (26), one can straightforwardly generalise Eq. (27) to relate the moments $\mathcal{E}_{2n}(t)$ of the partially transposed density matrix with the Rényi mutual information of various Rényi indices. In particular, introducing the ratio $\mathcal{R}_\alpha(t)$ as

$$\mathcal{R}_\alpha(t) := \ln \frac{\text{tr}[(\rho(t)_{AB}^{t_A})^\alpha]}{\text{tr}[(\rho(t)_{AB})^\alpha]} = \mathcal{E}_\alpha(t) - (1-\alpha)S_{AB}^{(\alpha)}(t), \quad (28)$$

we obtain the following universal relation that holds in the early-time regime (15)

$$\mathcal{R}_\alpha(t) \simeq \left(1 - \frac{\alpha}{2}\right) I_{A:B}^{(\alpha/2)}(t), \quad (29)$$

where we again analytically continued the result $2n \mapsto \alpha$. The moments $\mathcal{E}_\alpha(t)$, and the ratios $\mathcal{R}_\alpha(t)$ are not entanglement monotones, but yet they can still be used to detect entanglement [95, 96] and reveal universal aspects of many-body physics in various settings [46–49, 56, 97–99]. Importantly, in contrast to negativity, this quantities are currently experimentally accessible [95, 96].

One can gain intuition on Eq. (27) by considering Clifford circuits [100] — a subset of quantum circuits consisting of local unitary gates that maps a Pauli string to another Pauli string. Given a computational basis state of qubits on a 1d lattice evolved by a Clifford circuit, the time-evolved state at all times remains a stabiliser state, which satisfies a “structure theorem” [71, 101]. This ensures that using local Clifford unitaries acting on each of the subsystems, any stabiliser state defined on a tripartite system ABC can be decomposed to single-qubit product states, two-qubit Bell pair states with two qubits in two distinct regions, and three-qubit Greenberger-Horne-Zeilinger (GHZ) states with one qubit in each of A , B , and C . As correlation measures are invariant under local unitaries, the above decomposition allows for a simple expression of negativity and mutual information: the negativity between A and B is given by the number of Bell pairs (denoted by e_{AB}) shared between these two regions, i.e.,

$$\mathcal{E} = e_{AB} \ln 2, \quad (30)$$

while the mutual information between A and B is the sum of the quantum correlation resulting from the shared Bell pairs as well as the classical correlation resulting from the tripartite entanglement carried by the GHZ states among A , B , and C , i.e.,

$$\frac{1}{2}I_{A:B} = (e_{AB} + \frac{1}{2}g_{ABC}) \ln 2, \quad (31)$$

with g_{ABC} denoting the number of GHZ states. Due to the finite maximal speed of information spreading in local quantum circuits, building up non-vanishing connected correlation functions between any two of the three qubits located in A , B , and C , which is a defining feature of the three-qubit GHZ state, takes times $t > \min\{L_A, L_B, L_C\}/v_{\max}$. It follows that the GHZ-type tripartite correlation cannot exist in the early-time regime (15), and consequently, the correlation between any two subsystems solely results from entangled Bell

pairs. This justifies the correspondence between negativity and mutual information. Interestingly, the absence of tripartite entanglement has been suggested to be responsible for the correspondence (27) in certain equilibrium setting as well, see e.g., Ref. [102].

As mentioned in the introduction, the correspondence (27) has been first observed in non-interacting systems [64] (and its more general form (29) in [70]). Some important remarks, however, are in order. If one focuses on the leading order in time contribution, in non-interacting systems the correspondence holds also beyond the regime (15). Moreover, the negativity coincides with half of the mutual information also when the subsystems A and B are not adjacent, i.e., for a tripartition of the form $ACBC$, where the minimal separation between A and B is $d > 0$. While in both these cases the exact correspondence (27) ceases to hold for generic systems, it is interesting to ask whether it continues to be valid at leading order in time. This property could potentially distinguish different classes of dynamics (e.g., integrable vs chaotic).

Finally, we stress that the restriction to quantum circuits, i.e., to discrete space-time, is not essential for the validity of Eq. (27). Indeed, the only essential ingredient in our derivation is that the two edges of each subsystem are causally disconnected at early times because of the finite speed for the propagation of signals. Therefore we expect Eq. (27) to hold for any quantum many-body system where interactions are local enough to allow for a maximal speed for the propagation of signals. This include quantum spin-chains characterised by the Lieb-Robinson bound [103] (which can indeed be approximated by quantum circuits to arbitrary precision [104]), and relativistic quantum field theories. In addition, the same reasoning also suggests that Eq. (27) holds for systems without time-translation invariance in the setup of either local quantum circuits or unitary evolution driven by time-dependent local Hamiltonians.

Acknowledgments: We thank Tomaž Prosen and, especially, Pasquale Calabrese for very valuable comments on the manuscript and stimulating discussions. This work has been supported by the Royal Society through the University Research Fellowship No. 201101 (BB), by the EPSRC under grant EP/S020527/1 (KK), and Perimeter Institute for Theoretical Physics (TCL). Research at Perimeter Institute is supported in part by the Government of Canada through the Department of Innovation, Science and Economic Development and by the Province of Ontario through the Ministry of Colleges and Universities. BB and KK thank SISSA for hospitality in the early stage of this project.

[1] J. Eisert, M. Cramer, and M. B. Plenio, Colloquium: Area laws for the entanglement entropy, *Rev. Mod. Phys.* **82**, 277 (2010).

[2] U. Schollwöck, The density-matrix renormalization group in the age of matrix product states, *Ann. Physics* **326**, 96 (2011).

[3] J. I. Cirac, D. Pérez-García, N. Schuch, and F. Verstraete, Matrix product states and projected entangled

pair states: Concepts, symmetries, theorems, *Rev. Mod. Phys.* **93**, 045003 (2021).

[4] P. Calabrese and J. Cardy, Evolution of entanglement entropy in one-dimensional systems, *J. Stat. Mech.: Theory Exp.* **2005** (04), P04010.

[5] H. Liu and S. J. Suh, Entanglement tsunami: Universal scaling in holographic thermalization, *Phys. Rev. Lett.* **112**, 011601 (2014).

[6] M. Fagotti and P. Calabrese, Evolution of entanglement entropy following a quantum quench: Analytic results for the XY chain in a transverse magnetic field, *Phys. Rev. A* **78**, 010306 (2008).

[7] V. Alba and P. Calabrese, Entanglement and thermodynamics after a quantum quench in integrable systems, *Proc. Natl. Acad. Sci. U.S.A.* **114**, 7947 (2017).

[8] V. Alba, Entanglement and quantum transport in integrable systems, *Phys. Rev. B* **97**, 245135 (2018).

[9] A. M. Läuchli and C. Kollath, Spreading of correlations and entanglement after a quench in the one-dimensional Bose–Hubbard model, *J. Stat. Mech.: Theory Exp.* **2008** (05), P05018.

[10] H. Kim and D. A. Huse, Ballistic spreading of entanglement in a diffusive nonintegrable system, *Phys. Rev. Lett.* **111**, 127205 (2013).

[11] R. Pal and A. Lakshminarayanan, Entangling power of time-evolution operators in integrable and nonintegrable many-body systems, *Phys. Rev. B* **98**, 174304 (2018).

[12] A. Nahum, J. Ruhman, S. Vijay, and J. Haah, Quantum entanglement growth under random unitary dynamics, *Phys. Rev. X* **7**, 031016 (2017).

[13] A. Chan, A. De Luca, and J. T. Chalker, Solution of a minimal model for many-body quantum chaos, *Phys. Rev. X* **8**, 041019 (2018).

[14] B. Bertini, P. Kos, and T. Prosen, Entanglement spreading in a minimal model of maximal many-body quantum chaos, *Phys. Rev. X* **9**, 021033 (2019).

[15] L. Piroli, B. Bertini, J. I. Cirac, and T. Prosen, Exact dynamics in dual-unitary quantum circuits, *Phys. Rev. B* **101**, 094304 (2020).

[16] K. Klobas and B. Bertini, Entanglement dynamics in Rule 54: Exact results and quasiparticle picture, *SciPost Phys.* **11**, 107 (2021).

[17] A. Polkovnikov, K. Sengupta, A. Silva, and M. Vengalattore, Colloquium: Nonequilibrium dynamics of closed interacting quantum systems, *Rev. Mod. Phys.* **83**, 863 (2011).

[18] L. D’Alessio, Y. Kafri, A. Polkovnikov, and M. Rigol, From quantum chaos and eigenstate thermalization to statistical mechanics and thermodynamics, *Adv. Phys.* **65**, 239 (2016).

[19] C. Gogolin and J. Eisert, Equilibration, thermalisation, and the emergence of statistical mechanics in closed quantum systems, *Rep. Prog. Phys.* **79**, 056001 (2016).

[20] J. Eisert, M. Friesdorf, and C. Gogolin, Quantum many-body systems out of equilibrium, *Nat. Phys.* **11**, 124 (2015).

[21] P. Calabrese, F. H. L. Essler, and G. Mussardo, Introduction to ‘Quantum integrability in out of equilibrium systems’, *J. Stat. Mech.: Theory Exp.* **2016** (6), 064001.

[22] F. H. L. Essler and M. Fagotti, Quench dynamics and relaxation in isolated integrable quantum spin chains, *J. Stat. Mech.: Theory Exp.* **2016** (6), 064002.

[23] E. Ilievski, M. Medenjak, T. Prosen, and L. Zadnik, Quasilocal charges in integrable lattice systems, *J. Stat. Mech.: Theory Exp.* **2016** (6), 064008.

[24] F. Verstraete, J. J. García-Ripoll, and J. I. Cirac, Matrix product density operators: Simulation of finite-temperature and dissipative systems, *Phys. Rev. Lett.* **93**, 207204 (2004).

[25] M. Zwolak and G. Vidal, Mixed-state dynamics in one-dimensional quantum lattice systems: A time-dependent superoperator renormalization algorithm, *Phys. Rev. Lett.* **93**, 207205 (2004).

[26] J. Dubail, Entanglement scaling of operators: A conformal field theory approach, with a glimpse of simulability of long-time dynamics in 1+1d, *J. Phys. A* **50**, 234001 (2017).

[27] H. Wang and T. Zhou, Barrier from chaos: Operator entanglement dynamics of the reduced density matrix, *J. High Energ. Phys.* **2019** (12), 1.

[28] T. Prosen and M. Žnidarič, Is the efficiency of classical simulations of quantum dynamics related to integrability?, *Phys. Rev. E* **75**, 015202 (2007).

[29] J. Haegeman, J. I. Cirac, T. J. Osborne, I. Pižorn, H. Verschelde, and F. Verstraete, Time-dependent variational principle for quantum lattices, *Phys. Rev. Lett.* **107**, 070601 (2011).

[30] J. Haegeman, C. Lubich, I. Oseledets, B. Vandereycken, and F. Verstraete, Unifying time evolution and optimization with matrix product states, *Phys. Rev. B* **94**, 165116 (2016).

[31] E. Leviatan, F. Pollmann, J. H. Bardarson, D. A. Huse, and E. Altman, Quantum thermalization dynamics with matrix-product states, **1702.08894** (2017), arXiv:1702.08894.

[32] B. Kloss, Y. B. Lev, and D. Reichman, Time-dependent variational principle in matrix-product state manifolds: Pitfalls and potential, *Phys. Rev. B* **97**, 024307 (2018).

[33] C. D. White, M. Zaletel, R. S. K. Mong, and G. Refael, Quantum dynamics of thermalizing systems, *Phys. Rev. B* **97**, 035127 (2018).

[34] M. Žnidarič, Nonequilibrium steady-state Kubo formula: Equality of transport coefficients, *Phys. Rev. B* **99**, 035143 (2019).

[35] C. Krumnow, J. Eisert, and O. Legeza, Towards overcoming the entanglement barrier when simulating long-time evolution, **1904.11999** (2019), arXiv:1904.11999.

[36] T. Rakovszky, C. W. von Keyserlingk, and F. Pollmann, Dissipation-assisted operator evolution method for capturing hydrodynamic transport, *Phys. Rev. B* **105**, 075131 (2022).

[37] M. Schmitt and Z. Lenarčič, From observations to complexity of quantum states via unsupervised learning, **arXiv:2102.11328** (2021), arXiv:2102.11328.

[38] I. Reid and B. Bertini, Entanglement barriers in dual-unitary circuits, *Phys. Rev. B* **104**, 014301 (2021).

[39] T. Prosen and I. Pižorn, Operator space entanglement entropy in a transverse Ising chain, *Phys. Rev. A* **76**, 032316 (2007).

[40] I. Pižorn and T. Prosen, Operator space entanglement entropy in XY spin chains, *Phys. Rev. B* **79**, 184416 (2009).

[41] A. Peres, Separability criterion for density matrices, *Phys. Rev. Lett.* **77**, 1413 (1996).

[42] J. Eisert and M. B. Plenio, A comparison of entanglement measures, *J. Mod. Opt.* **46**, 145 (1999).

[43] M. Horodecki, P. Horodecki, and R. Horodecki, Sepa-

rability of n-particle mixed states: Necessary and sufficient conditions in terms of linear maps, *Phys. Lett. A* **283**, 1 (2001).

[44] G. Vidal and R. F. Werner, Computable measure of entanglement, *Phys. Rev. A* **65**, 032314 (2002).

[45] M. B. Plenio, Logarithmic negativity: A full entanglement monotone that is not convex, *Phys. Rev. Lett.* **95**, 090503 (2005).

[46] P. Calabrese, J. Cardy, and E. Tonni, Entanglement negativity in quantum field theory, *Phys. Rev. Lett.* **109**, 130502 (2012).

[47] P. Calabrese, J. Cardy, and E. Tonni, Entanglement negativity in extended systems: A field theoretical approach, *J. Stat. Mech.: Theory Exp.* **2013** (02), P02008.

[48] V. Alba, Entanglement negativity and conformal field theory: A Monte Carlo study, *J. Stat. Mech.: Theory Exp.* **2013** (05), P05013.

[49] C.-M. Chung, V. Alba, L. Bonnes, P. Chen, and A. M. Läuchli, Entanglement negativity via the replica trick: A quantum Monte Carlo approach, *Phys. Rev. B* **90**, 064401 (2014).

[50] P. Calabrese, J. Cardy, and E. Tonni, Finite temperature entanglement negativity in conformal field theory, *J. Phys. A: Math. Theor.* **48**, 015006 (2014).

[51] P. Ruggiero, V. Alba, and P. Calabrese, Negativity spectrum of one-dimensional conformal field theories, *Phys. Rev. B* **94**, 195121 (2016).

[52] Y. A. Lee and G. Vidal, Entanglement negativity and topological order, *Phys. Rev. A* **88**, 042318 (2013).

[53] X. Wen, S. Matsuura, and S. Ryu, Edge theory approach to topological entanglement entropy, mutual information, and entanglement negativity in Chern-Simons theories, *Phys. Rev. B* **93**, 245140 (2016).

[54] X. Wen, P.-Y. Chang, and S. Ryu, Topological entanglement negativity in Chern-Simons theories, *J. High Energ. Phys.* **2016** (9), 12.

[55] O. Hart and C. Castelnovo, Entanglement negativity and sudden death in the toric code at finite temperature, *Phys. Rev. B* **97**, 144410 (2018).

[56] T.-C. Lu, T. H. Hsieh, and T. Grover, Detecting topological order at finite temperature using entanglement negativity, *Phys. Rev. Lett.* **125**, 116801 (2020).

[57] P. K. Lim, H. Asasi, J. C. Y. Teo, and M. Mulligan, Disentangling (2+1)D topological states of matter with entanglement negativity, *Phys. Rev. B* **104**, 115155 (2021).

[58] T.-C. Lu and S. Vijay, Characterizing long-range entanglement in a mixed state through an emergent order on the entangling surface, **2201.07792** (2022), arXiv:2201.07792.

[59] A. Coser, E. Tonni, and P. Calabrese, Entanglement negativity after a global quantum quench, *J. Stat. Mech.: Theory Exp.* **2014** (12), P12017.

[60] V. Eisler and Z. Zimborás, Entanglement negativity in the harmonic chain out of equilibrium, *New J. Phys.* **16**, 123020 (2014).

[61] X. Wen, P.-Y. Chang, and S. Ryu, Entanglement negativity after a local quantum quench in conformal field theories, *Phys. Rev. B* **92**, 075109 (2015).

[62] M. Hoogeveen and B. Doyon, Entanglement negativity and entropy in non-equilibrium conformal field theory, *Nucl. Phys. B* **898**, 78 (2015).

[63] J. Kudler-Flam, H. Shapourian, and S. Ryu, The negativity contour: A quasi-local measure of entanglement for mixed states, *SciPost Phys.* **8**, 63 (2020).

[64] V. Alba and P. Calabrese, Quantum information dynamics in multipartite integrable systems, *EPL* **126**, 60001 (2019).

[65] M. J. Gullans and D. A. Huse, Entanglement structure of current-driven diffusive fermion systems, *Phys. Rev. X* **9**, 021007 (2019).

[66] M. Gruber and V. Eisler, Time evolution of entanglement negativity across a defect, *J. Phys. A: Math. Theor.* **53**, 205301 (2020).

[67] T.-C. Lu and T. Grover, Entanglement transitions as a probe of quasiparticles and quantum thermalization, *Phys. Rev. B* **102**, 235110 (2020).

[68] B. Shi, X. Dai, and Y.-M. Lu, Entanglement negativity at the critical point of measurement-driven transition, **2012.00040** (2020), arxiv:2012.00040.

[69] J. Kudler-Flam, Y. Kusuki, and S. Ryu, The quasiparticle picture and its breakdown after local quenches: Mutual information, negativity, and reflected entropy, *J. High Energ. Phys.* **2021** (3), 1.

[70] S. Murciano, V. Alba, and P. Calabrese, Quench dynamics of Rényi negativities and the quasiparticle picture, **2110.14589** (2021), arXiv:2110.14589.

[71] S. Sang, Y. Li, T. Zhou, X. Chen, T. H. Hsieh, and M. P. A. Fisher, Entanglement negativity at measurement-induced criticality, *PRX Quantum* **2**, 030313 (2021).

[72] Z. Weinstein, Y. Bao, and E. Altman, Measurement-induced power law negativity in an open monitored quantum circuit, **2202.12905** (2022), arXiv:2202.12905.

[73] M. C. Bañuls, M. B. Hastings, F. Verstraete, and J. I. Cirac, Matrix-product states for dynamical simulation of infinite chains, *Phys. Rev. Lett.* **102**, 240603 (2009).

[74] A. Müller-Hermes, J. I. Cirac, and M. C. Bañuls, Tensor network techniques for the computation of dynamical observables in one-dimensional quantum spin systems, *New J. Phys.* **14**, 075003 (2012).

[75] M. B. Hastings and R. Mahajan, Connecting entanglement in time and space: Improving the folding algorithm, *Phys. Rev. A* **91**, 032306 (2015).

[76] M. Frías-Pérez and M. C. Bañuls, Light cone tensor network and time evolution, **2201.08402** (2022), arXiv:2201.08402.

[77] M. Akila, D. Waltner, B. Gutkin, and T. Guhr, Particle-time duality in the kicked Ising spin chain, *J. Phys. A: Math. Theor.* **49**, 375101 (2016).

[78] B. Bertini, P. Kos, and T. Prosen, Exact spectral form factor in a minimal model of many-body quantum chaos, *Phys. Rev. Lett.* **121**, 264101 (2018).

[79] B. Bertini, P. Kos, and T. Prosen, Exact correlation functions for dual-unitary lattice models in 1+1 dimensions, *Phys. Rev. Lett.* **123**, 210601 (2019).

[80] A. Chan, A. De Luca, and J. T. Chalker, Spectral Lyapunov exponents in chaotic and localized many-body quantum systems, *Phys. Rev. Research* **3**, 023118 (2021).

[81] S. J. Garratt and J. T. Chalker, Local pairing of Feynman histories in many-body Floquet models, *Phys. Rev. X* **11**, 021051 (2021).

[82] S. J. Garratt and J. T. Chalker, Many-body delocalization as symmetry breaking, *Phys. Rev. Lett.* **127**, 026802 (2021).

[83] M. Ippoliti and V. Khemani, Postselection-free entanglement dynamics via spacetime duality, *Phys. Rev.*

Lett. **126**, 060501 (2021).

[84] T.-C. Lu and T. Grover, Spacetime duality between localization transitions and measurement-induced transitions, *PRX Quantum* **2**, 040319 (2021).

[85] M. Ippoliti, T. Rakovszky, and V. Khemani, Fractal, logarithmic, and volume-law entangled nonthermal steady states via spacetime duality, *Phys. Rev. X* **12**, 011045 (2022).

[86] K. Klobas and B. Bertini, Exact relaxation to Gibbs and non-equilibrium steady states in the quantum cellular automaton Rule 54, *SciPost Phys.* **11**, 106 (2021).

[87] K. Klobas, B. Bertini, and L. Piroli, Exact thermalization dynamics in the “Rule 54” quantum cellular automaton, *Phys. Rev. Lett.* **126**, 160602 (2021).

[88] G. Giudice, G. Giudici, M. Sonner, J. Thoenness, A. Leroose, D. A. Abanin, and L. Piroli, Temporal entanglement, quasiparticles and the role of interactions, [2112.14264](https://arxiv.org/abs/2112.14264) (2021), arXiv:2112.14264.

[89] A. Bobenko, M. Bordemann, C. Gunn, and U. Pinkall, On two integrable cellular automata, *Commun. Math. Phys.* **158**, 127 (1993).

[90] B. Buča, K. Klobas, and T. Prosen, Rule 54: Exactly solvable model of nonequilibrium statistical mechanics, *J. Stat. Mech.: Theory Exp.* **2021** (7), 074001.

[91] A. Leroose, M. Sonner, and D. A. Abanin, Influence matrix approach to many-body Floquet dynamics, *Phys. Rev. X* **11**, 021040 (2021).

[92] A. Leroose, M. Sonner, and D. A. Abanin, Scaling of temporal entanglement in proximity to integrability, *Phys. Rev. B* **104**, 035137 (2021).

[93] M. Sonner, A. Leroose, and D. A. Abanin, Influence functional of many-body systems: Temporal entanglement and matrix-product state representation, *Ann. Physics* **435**, 168677 (2021).

[94] M. Sonner, A. Leroose, and D. A. Abanin, Characterizing many-body localization via exact disorder-averaged quantum noise, *Phys. Rev. B* **105**, L020203 (2022).

[95] A. Elben, R. Kueng, H. Y. R. Huang, R. van Bijnen, C. Kokail, M. Dalmonte, P. Calabrese, B. Kraus, J. Preskill, P. Zoller, and B. Vermersch, Mixed-state entanglement from local randomized measurements, *Phys. Rev. Lett.* **125**, 200501 (2020).

[96] A. Neven, J. Carrasco, V. Vitale, C. Kokail, A. Elben, M. Dalmonte, P. Calabrese, P. Zoller, B. Vermersch, R. Kueng, and B. Kraus, Symmetry-resolved entanglement detection using partial transpose moments, *npj Quantum Inf.* **7**, 152 (2021).

[97] P. Calabrese, L. Tagliacozzo, and E. Tonni, Entanglement negativity in the critical Ising chain, *J. Stat. Mech.: Theory Exp.* **2013** (05), P05002.

[98] K.-H. Wu, T.-C. Lu, C.-M. Chung, Y.-J. Kao, and T. Grover, Entanglement Rényi negativity across a finite temperature transition: A Monte Carlo study, *Phys. Rev. Lett.* **125**, 140603 (2020).

[99] E. Wybo, M. Knap, and F. Pollmann, Entanglement dynamics of a many-body localized system coupled to a bath, *Phys. Rev. B* **102**, 064304 (2020).

[100] D. Gottesman, Class of quantum error-correcting codes saturating the quantum Hamming bound, *Phys. Rev. A* **54**, 1862 (1996).

[101] S. Bravyi, D. Fattal, and D. Gottesman, GHZ extraction yield for multipartite stabilizer states, *J. Math. Phys.* **47**, 062106 (2006).

[102] H. Shapourian, S. Liu, J. Kudler-Flam, and A. Vishwanath, Entanglement negativity spectrum of random mixed states: A diagrammatic approach, *PRX Quantum* **2**, 030347 (2021).

[103] E. H. Lieb and D. W. Robinson, The finite group velocity of quantum spin systems, in *Statistical mechanics*, edited by B. Nachtergael, J. P. Solovej, and J. Yngvason (Springer, 1972) pp. 425–431.

[104] T. J. Osborne, Efficient approximation of the dynamics of one-dimensional quantum spin systems, *Phys. Rev. Lett.* **97**, 157202 (2006).